國 立 交 通 大 學

電子工程學系電子研究所

碩 士 論 文

鎳鐵與氧化鋁奈米複合材料的合成及製程開發使螺旋電感的性能增強

Material Synthesis and Process Development of NiFe-AAO

Nanocomposite for Performance Enhancement of On-chip Spiral

Inductor

研 究 生：許欣富

指導教授：鄭裕庭　教授

中 華 民 國 九 十 八 年 九 月
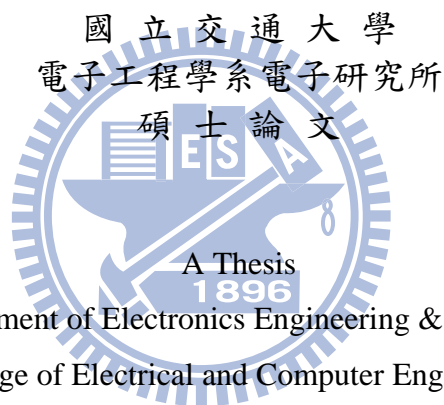
鎳鐵與氧化鋁奈米複合材料的合成及製程開發使螺旋電感的性能增強

Material Synthesis and Process Development of NiFe-AAO Nanocomposite for Performance Enhancement of On-chip Spiral Inductor

研 究 生：許欣富　　　　Student：Hsin-Fu Hsu

指導教授：鄭裕庭　　　　Advisor：Yu-Ting Cheng

國 立 交 通 大 學
電子工程學系電子研究所
碩 士 論 文

A Thesis

Submitted to Department of Electronics Engineering & Institute of Electronics

College of Electrical and Computer Engineering

National Chiao Tung University

in partial Fulfillment of the Requirements

for the Degree of

Master

in

Electronics Engineering

Sep 2009

Hsinchu, Taiwan, Republic of China

中華民國九十八年九月

鎳鐵與氧化鋁奈米複合材料的合成及製程開發使螺旋電感的性能增強

學生：許欣富　　　　　　　　　　　　　　指導教授：鄭裕庭 教授

國立交通大學電子工程學系暨電子研究所碩士班

摘　　　要

在此篇論文中，我們使用奈米鎳鐵柱應用於高頻螺旋電感，利用空間中相對磁導率的提升來增加電感值，以達到無線通訊應用晶片面積微小化的目標。直徑 70nm，高度 1μm 的奈米鎳鐵柱是利用沉積在矽基板上的陽極氧化鋁模板以電鍍方法所製成，規則的奈米鎳柱陣列被高電阻率的陽極氧化鋁模板所分隔，有效的避免了電感在高頻應用時所產生在磁性材料的渦電流損耗。在本實驗設計中，奈米鎳柱應用於螺旋電感，觀察奈米鎳柱鐵芯受到電感均勻的磁場磁化下，所得到的奈米鎳柱鐵芯電感高頻特性。最後，已完成的四圈半奈米鎳柱鐵芯螺旋電感的高頻特性被量測由 0.1GHz 到 5GHz，電感值約有 23 % 的增加，持續到達 1GHz 為止。
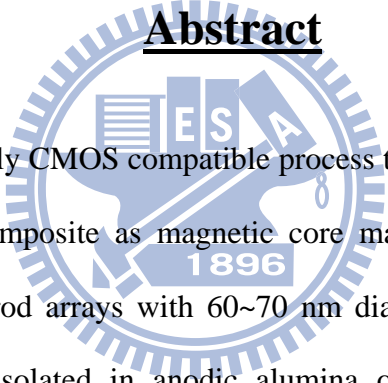
Material Synthesis and Process Development of NiFe-AAO Nanocomposite for Performance Enhancement of On-chip Spiral Inductor

Student：Hsin-Fu Hsu   Advisor：Dr. Yu-Ting Cheng

Department of Electronics Engineering & Institute of Electronics
National Chiao Tung University

Abstract

This thesis presented a fully CMOS compatible process to implement NiFe (68 at%. Ni and 32 at.% Fe) –AAO nanocomposite as magnetic core material for on-chip spiral inductor fabrication. The NiFe nanorod arrays with 60~70 nm diameter using DC electroplated are deposited and electrically isolated in anodic alumina oxide (AAO) template on silicon substrate. Experimental results show that the spiral inductor of 4.5 turns using NiFe-AAO nanocomposite magnetic core can have 23% inductance enhancement than that of inductor without the core up to 1 GHz.

誌　　　謝

Contents

Figure Captions

Chapter1

Chapter 2

Chapter 3

Table Captions

Chapter 1

Chapter 2

Chapter 3

Chapter 1 Introduction

One of the technical challenges in the cost reduction of RFIC (Radio Frequency Integrated Circuit) for consumer electronic applications is inevitable large area occupation of RF on-chip passive components, such as inductor, capacitor, and filter...etc. For instance, inductor for GHz RFIC operation ranging from 1.5 to 3.5 nH can have the size of 0.06 to 0.08 μm^2 [1]. The larger size the inductor is, the higher inductance it can have. In addition, it is required to have least three inductors for a second order bandpass filter design whose size will be up to 0.62 mm^2 at least [2]. Thus, high-k and ferromagnetic materials have been synthesized and developed to increase the capacitance and inductance per area, respectively, in the development of radio frequency integrated circuit (RFIC) technology in recent years. In this thesis, a new ferromagnetic composite material is synthesized for enhancing inductor performance.

Previously, Viala *et al*. demonstrated the coplanar ferromagnetic inductor with a 15% increase in inductance using solid magnetic (CoZrNb) alloy [3]. Kim *et al*. proposed on-chip solenoid inductors incorporated with Fe_3O_4 magnetite nanorod cores for having higher inductance [4]. Jiang *et al*. employed exchange-coupled characteristic of antiferromagnetic/ferromagnetic multilayers (IrMn/CoFe) to enhance inductance up to 20% without having any Q preference degradation [5]. Table 1-1 introduces these approaches about the inductors with magnetic material core in RF range application. Although these approaches can indeed achieve the inductance enhancement, the enhancement which only occurs in MHz range and is realized with CMOS-incompatible material and processes is not practical in real CMOS on-chip spiral inductor fabrication. Thus, our group

developed a new composite material with CMOS compatible fabrication process that is electroless deposited Ni-AAO (anodic alumina oxide) nanocomposite. Using the composite as magnetic core material, inductance enhancement can be realized up to 5.3 GHz [6]. Fig.1. shows the representation of the 3.5turns spiral inductors with the Ni Nanorods core.
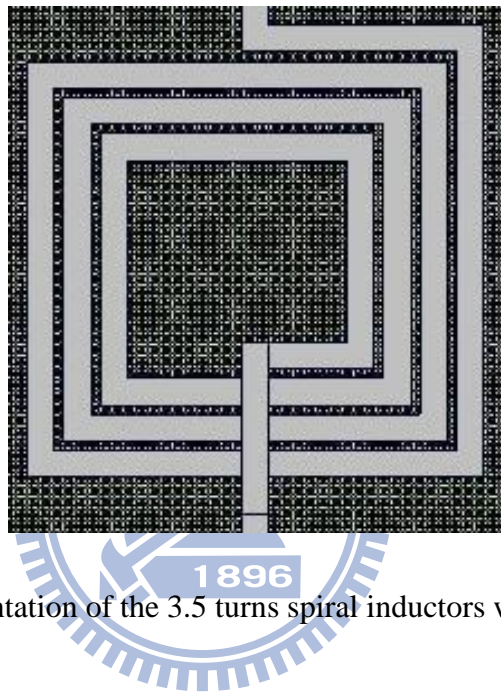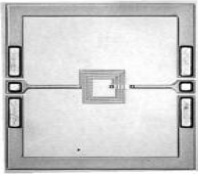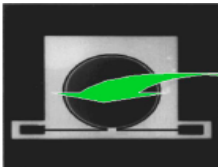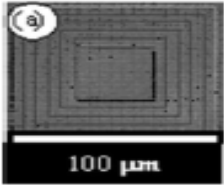
Fig.1-1.Schematic representation of the 3.5 turns spiral inductors with the Ni nanorods core
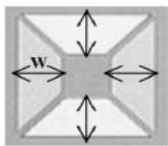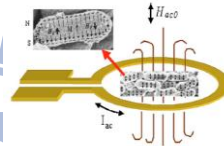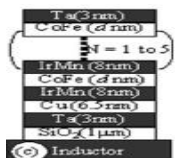
Nevertheless, it has been found that such an electroless Ni-P alloy has strong relation to its *P* content in terms of magnetic property and the saturated magnetization of Ni-P is less than that of a pure Ni [7]. According to Weiss theory [8], *P* incorporation would result in the interatomic distance enlargement of Ni which can cause exchange force reduction. Since the force reduction would make the permeability of Ni-P smaller than that of pure Ni [7], only 3% inductance enhancement is observed so far in the inductor using the Ni-AAO nanocomposite as the magnetic core. Meanwhile, ferromagnetic resonance (FMR) frequency (FMR) is expressed as $\gamma/2\pi[H_k(H_k + 4\pi M_s)]$, where γ is the gyromagnetic ratio, H_k is the anisotropy magnetic field, and M_s is the saturation

magnetization. To effectively elevate the FMR frequency well above several gigahertz ranges for practical application to RFIC using the inductor with ferromagnetic core, it is required further study to improve material characteristics such as H_k and M_s.

Previous study has shown that the rod like shape and nanometer size of magnetic material could have higher anisotropy field H_k [9]. Thus, in this thesis, a NiFe-AAO nanocomposite with fully CMOS-compatible process will be developed for on-chip spiral inductors fabrication. Because NiFe has larger permeability and saturation magnetization than that of Ni and has a form of nanorod in the composite system, material characterization, better inductor performance can be expected.

Table.1-1.The introduction of some ferromagnetic inductor approaches.

	RF plane ferromagnetic inductors on silicon (2004) [3]	Magnetite (Fe3O4) nanorod cores for Integrated Solenoid RF Inductors (2006) [4]	Exchange-Coupled IrMn/CoFe Mulitayers for RF Integrated Inductors (2007) [5]
L enhancement (%) @ application frequency	L = 4.2nH (+15%) at 1.2GHz	L = 2.63nH (+3.5%) at 3GHz	L = 3.8nH (+30%) at 1.8GHz
Q variation (%) @ useful frequency	Q = 10 (-35%) at 1GHz	Q = 2.9 (-3%) at 3GHz	Q = 6.5 (+0%) at 1.8GHz

Q peak variation @ frequency	Q = 23 at 5GHz ⇩ Q = 11 at 1.2GHz	Q = 9.5 at 13GHz ⇩ Q = 7 at 11GHz	Q = 6.3 at 2GHz ⇩ Q = 6.3 at 1.7GHz
(f_{FMR}) Ferromagnetic resonance frequency	2.5GHz (strong absorbability)	5GHz (weak absorbability)	4.3GHz (strong absorbability)
Air core (f_{Lc}) Self-resonant Frequency	N/A ~ (>8GHz)	17GHz	5GHz
Magnetic material	CoZrNb	Fe_3O_4 nanorod	CoFe
Structure and design	Solid magnetic plane	Magnetic material in core	IrMn/CoFe Mulitayers
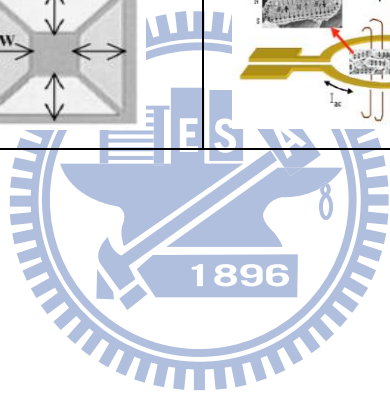
Chapter 2 Experimental Setup

2.1 NiFe-AAO Nanocomposite Synthesis and Characterization

In comparison with the previous developed electroless deposited Ni-AAO nanocomposite process, the synthesis of NiFe-AAO nanocomposite requires a seed layer under AAO layer. Thus, a Ti (200 nm)/Al (1000 nm) layer is e-beam deposited on a 4" silicon substrate grown with a layer of 0.2 um thermal oxide as electrical isolation layer. Then, the AAO template is fabricated by applying a constant voltage 40V to the substrate in a 0.3 M oxalic acid ($H_2C_2O_4$) solution at 2℃. The low temperature anodization process can reduce excessive current flow and heat evolution to make the AAO with the characteristics of small-pore films [12]. Fig.2-1. shows the process flow.

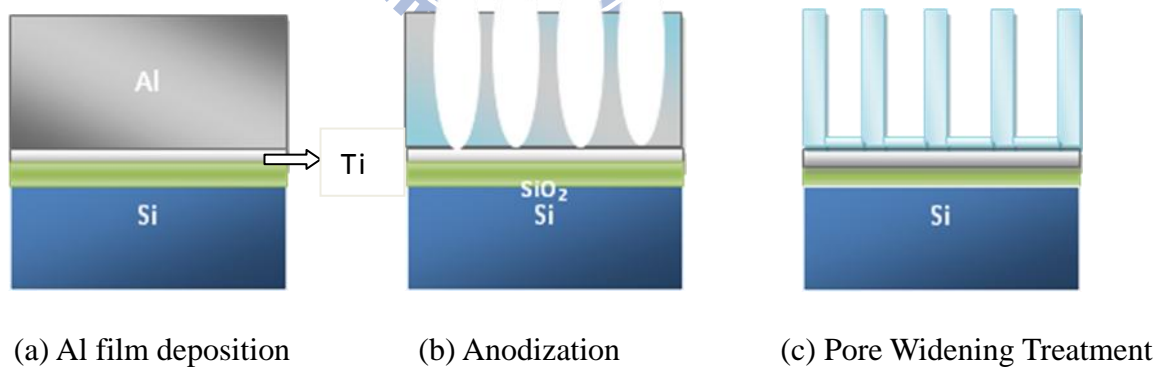| (a) Al film deposition | (b) Anodization | (c) Pore Widening Treatment |

Fig.2-1. Anodization process flow.

Once the film is anodized, the voltage is reduced from 40V to 15V with a rate of 0.11V/s and then kept for 15mins for thinning the alumina oxide barrier layer. The insulting barrier layer is then further thinned to completely anodized Al film by applied a reversed-bias voltage (-2.2V) to the substrate in a 0.5M saturated

KCL at 2°C for 10mins [12, 13]. Finally, the AAO temple is put in a 5% H_3PO_4 solution at 30°C for 25mins to form a uniformly distributed nanopore structure with the size of 70 nm in diameter, shown in Fig.2-2.

15.0kV 12.2mm ×45.0k SE(U)   1.00um
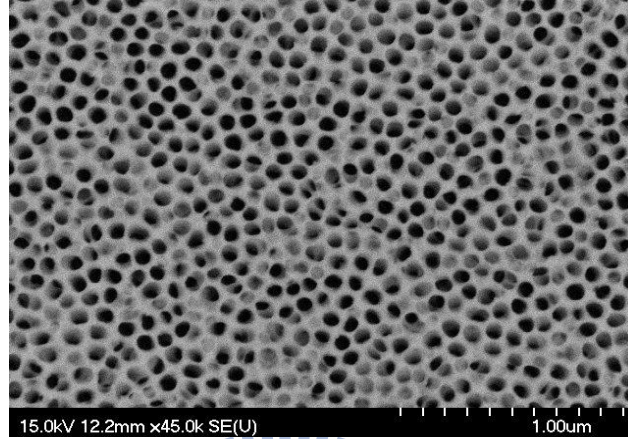
Fig.2-2. The SEM image of AAO template with 70 nm pore diameter.

For the synthesis of NiFe-AAO nanocomposite, the as-fabricated AAO temple is DC electroplated in a Ni sulfate based NiFe bath with the formulation listed in Table 2-1 [14]. The plating conditions are 28°C and 0.035A/mm^2 current density. Fig. 2-3 shows the as-deposited NiFe-AAO nanocomposite. NiFe nanorods are grown within the AAO matrix. Fig.2-4. shows the superconducting quantum interference device (SQUID) measurements of NiFe-AAO nanocomposite; the applied field directions are in plane and out plane. The slope of the M-H curve exhibits the relative permeability, the larger slope lead to the larger permeability. The relative permeability can be calculated as follows:

$$\mu_r = 1 + {4\pi M}/{H_o} \tag{1}$$

where M is magnetization and H_0 is the applied magnetic field. The relative permeability in our case are 1.66 in out-plane applied field and 20.3 in in-plane

applied field (at 100 Oe). In addition, the FMR frequency of ferromagnetic film is estimated about as high as 5.72 GHz due to large H_k, which is about 800 Oe.

Table 2-1
Characteristics of NiFe electrolyte

Compound	Concentration
Nickel sulfate (g/l)	200
Iron sulfate (g/l)	8
Nickel chloride (g/l)	5
Boric acid (g/l)	25
Saccharin (g/l)	2
Sodium lauryl sulfate 1 cm (g/l)	0.1
Deposition temperature (℃)	28
PH	3

15.0kV 14.0mm ×40.0k SE(U)   1.00um

(a)

15.0kV 14.8mm ×35.0k SE(U)   1.00um
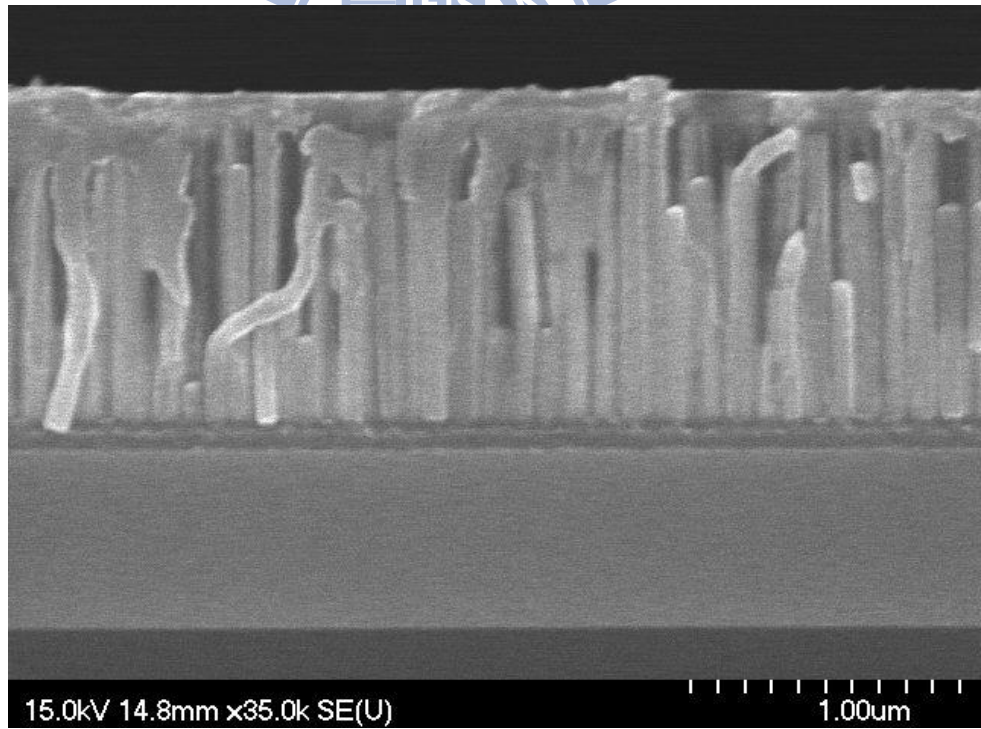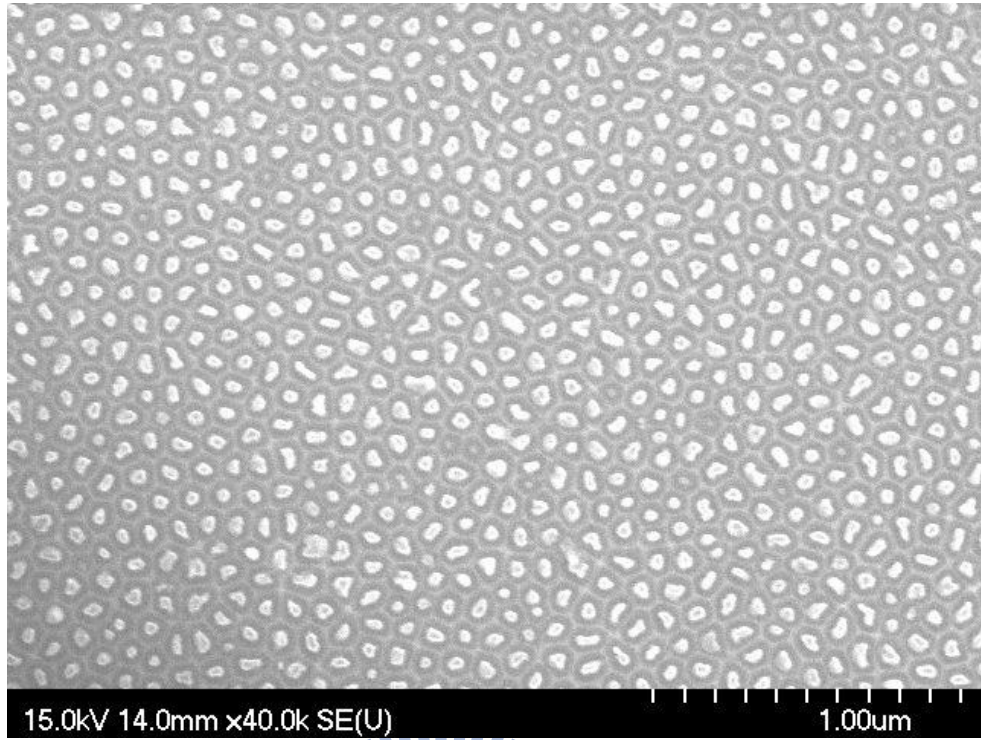
(b)

Fig.2-3. SEM photographs of NiFe Nanorods of (a) top view (b) cross section.

(a)
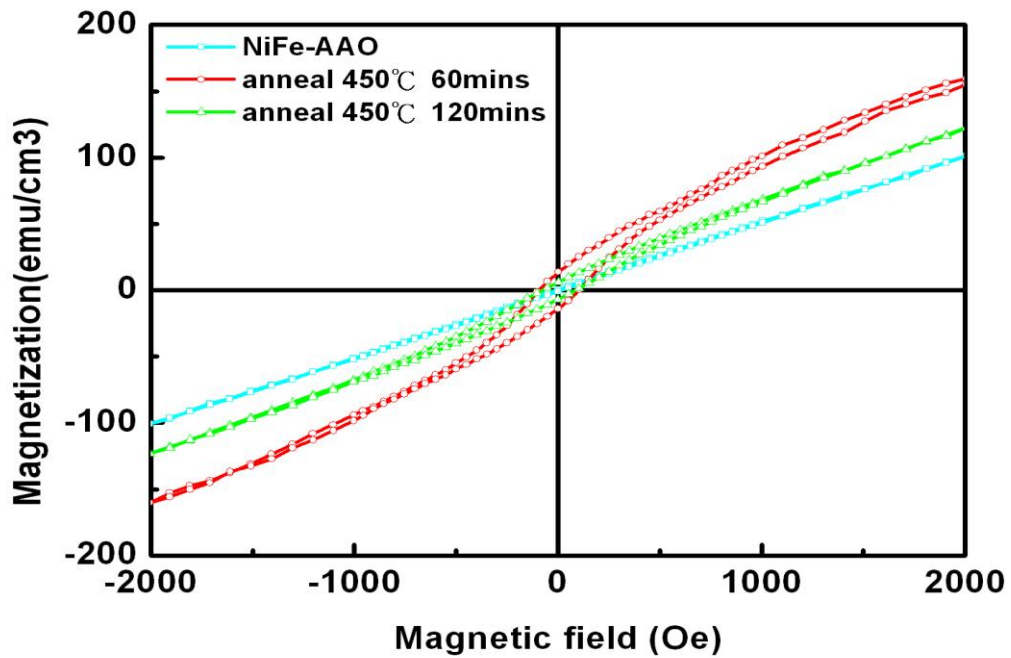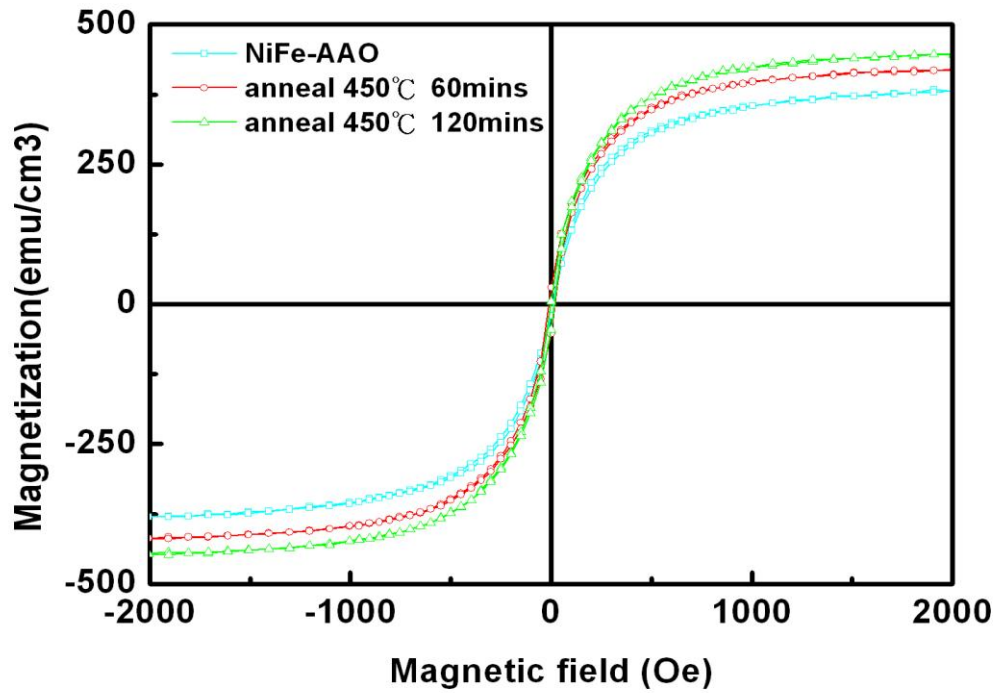
(b)

Fig. 2-4. M-H loops of NiFe-AAO nanocomposite with different form of applied magnetic fields. (a) in-plane. (b) out-of-plane.

2.2 Inductor Fabrication

The spiral inductors of 3.5 and 4.5 turns, that are made of 5-um-thick electroplated Cu and designed with 100 um in inner diameter, 15 um in line width, and 5 um in line space have been utilized for the investigation of inductance enhancement using NiFe-AAO nanocomposite as a magnetic core. Fig.5 illustrates the fabrication process of the on–chip spiral inductors with NiFe nanorods. It begins with wet oxidation at 1050℃ for 0.75 um of thermal oxide, followed by electron-beam-evaporated Ti/Al (0.2 um/1um) deposition on the p-type silicon substrate as shown in Fig.2-5(a), and then AAO template is fabricated using the aforementioned as shown in Fig.2-5(b). The NiFe nanorod arrays were then deposited by DC electroplating shown in Fig.2-5(c). Once the magnetic layer is fabricated, as Fig.2-5(d) shows, a layer of 0.2-um-thick-SiO_2 is sputtered on the top of the composite film as an electrical insulation layer followed by the first thin Cr/Cu (500Å /1000Å) adhesion/seed layer deposition. For the inductor fabrication, a 6um thick AZ 4620 photo-resist is patterned to define the region for coil fabrication of spiral inductor, as shown in Fig.2-5(e). After the first layer of 5-um-thick Cu plating, another 10um thick AZ 4620 is spun, patterned, and sputtered with 150nm Cu seed layer for the via filling of Cu as shown in Fig.2-5(f). Fig.2-5(g) shows another 10-um AZ 4620 is spun onto the plated structure, patterned, and plated with 5um-thick Cu to define air bridge after via filling. At final, the fabrication of the spiral inductor is done right after the Cu seed layer removal, which is chemically etched away using Cu and Cr etchants as shown in Fig.2-5(h). Fig.2-6. shows an as-fabricated 3.5-turn spiral inductor with magnetic

NiFe-AAO nanocomposite core.

(a)

(b)

(c)

(d)

(e)

(f)

(g)

(h)

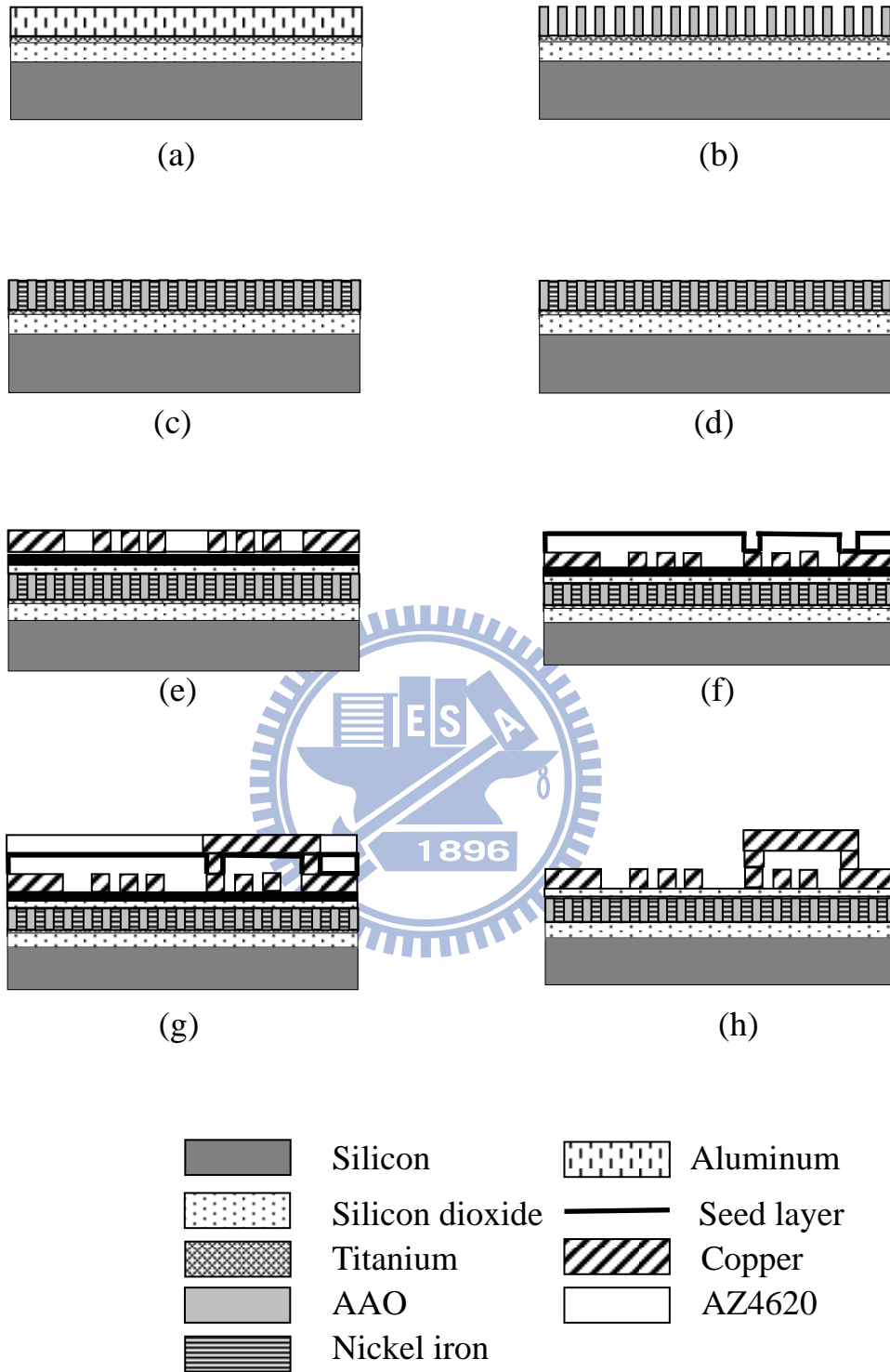|	Silicon		Aluminum
	Silicon dioxide	—	Seed layer
	Titanium		Copper
	AAO		AZ4620
	Nickel iron		

Fig.2-5 Schematic of the inductors with the NiFe nanorods core fabrication processes.
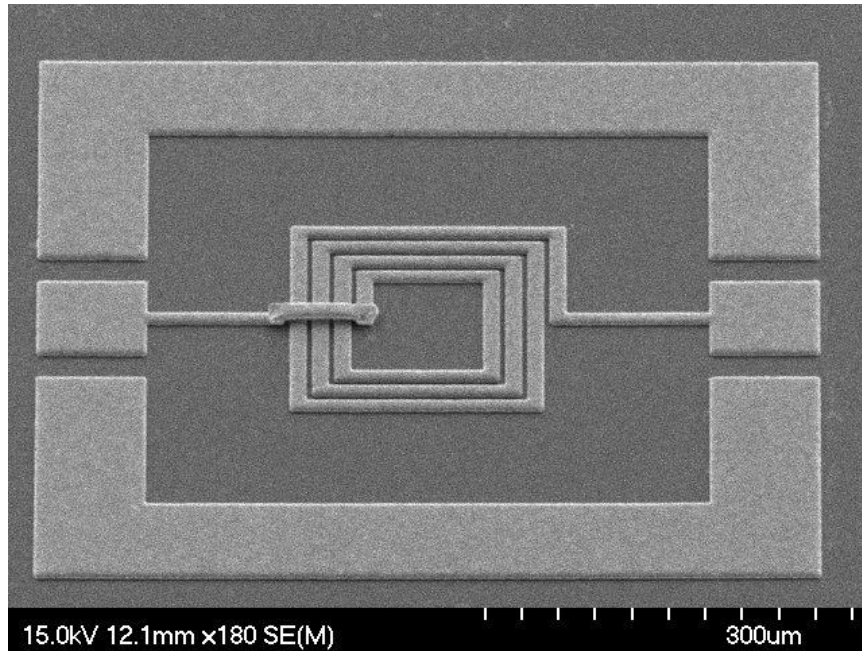
Fig.2-6 SEM photograph of as-fabricated on chip spiral inductors with NiFe-AAO nanocomposite.

Chapter 3 Measurement and discussion

In the experiment, the two-port S-parameters of the inductors are measured in the frequency range of 0.5 to 5 GHz with an on-wafer probe station using the high- frequency probes (Cascade Microtech, Inc., ACP-40-GSG-100μm) and Agilent E8364B PNA network analyzer. After short-open-load-through (SOLT) calibration then we can measured the S-parameters. The parasitic parallel capacitance and series contact resistance between the substrate and the contact pads of the inductor are de-embedded via the measurement using well-designed dummy patterns [1]. The de-embedded S parameters are then transformed into Y-parameter using Agilent ADS software. The equivalent series inductance (L) and quality factor (Q) of the inductors are extracted from the Y-parameters base on the following equation [14], respectively:

$$L = \text{Im}(1/Y_{11})/2\,\pi\,f \qquad\qquad (3)$$

$$Q = \text{Im}(1/Y_{11})/\text{Re}(1/Y_{11}) \qquad\qquad (4)$$

where f is the signal frequency.

The frequency-dependent inductance and Q-factor of the fabricated inductors are depicted in Fig.3-1(a) and (b) shows that the spiral inductor of 3.5 turns with NiFe-AAO nanocomposite magnetic core can have 25% inductance enhancement than that of inductor without the core up to 1 GHz. Meanwhile, the maximum Q-factor (Q_m) decreases from 12 to 6 at 1 GHz, which is about 50% reduction. Similar inductance enhancement and Q degradation also occur in the

case of the spiral inductor of 4.5 turns. The spiral inductor of 4.5 turns with NiFe-AAO nanocomposite magnetic core can have 23% inductance enhancement than that of inductor without the core up to 1 GHz but the Q decreases from 10.3 to 6.4 at 1 GHz, which is about 38% reduction.

In Fig.3-1 (a) and (c), the spiral inductor with NiFe-AAO nanocomposite magnetic core has a capacitance curve trend and has a worse Q-factor than that of inductor without the magnetic core because of the titanium, in the bottom of NiFe-AAO. Titanium is used as the seed layer for NiFe electroplating, but it would result in the effect of parasitic capacitance increase and eddy current loss on the layer of Ti that further cause poor inductance and Q performance. Therefore, it is critical to eliminate the effect resulted by the Ti layer. Previously, *H.H et al.* proposed thermal anneal at the temperature higher than 450 ℃ can make the formation of an amorphous layer at the interface between the Ti and the SiO₂. According to the O concentration profile determined by SIMS, it suggested that this layer was mainly TiO_x [15], shown in Fig.3-2.
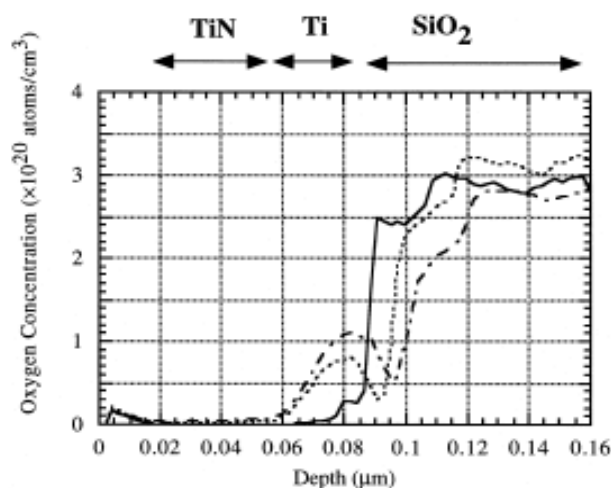
Fig.3-2. The O concentration profile determined by SIMS.
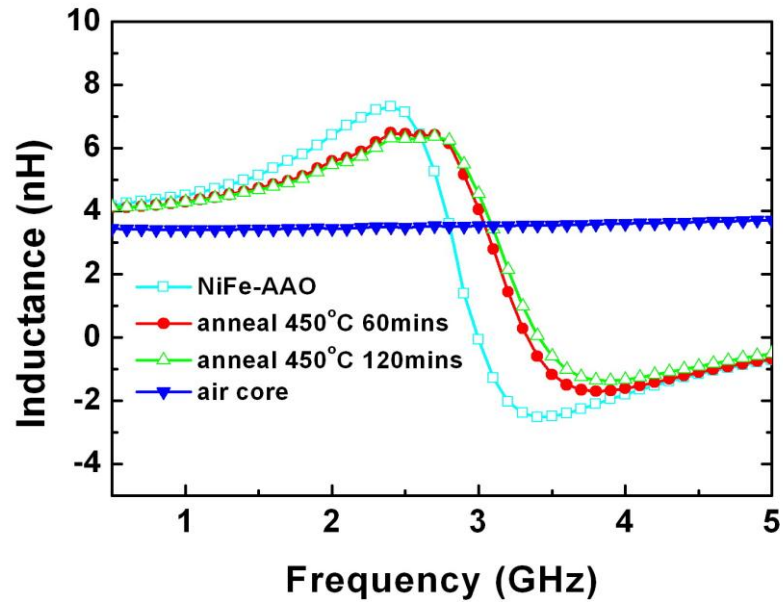
(a)
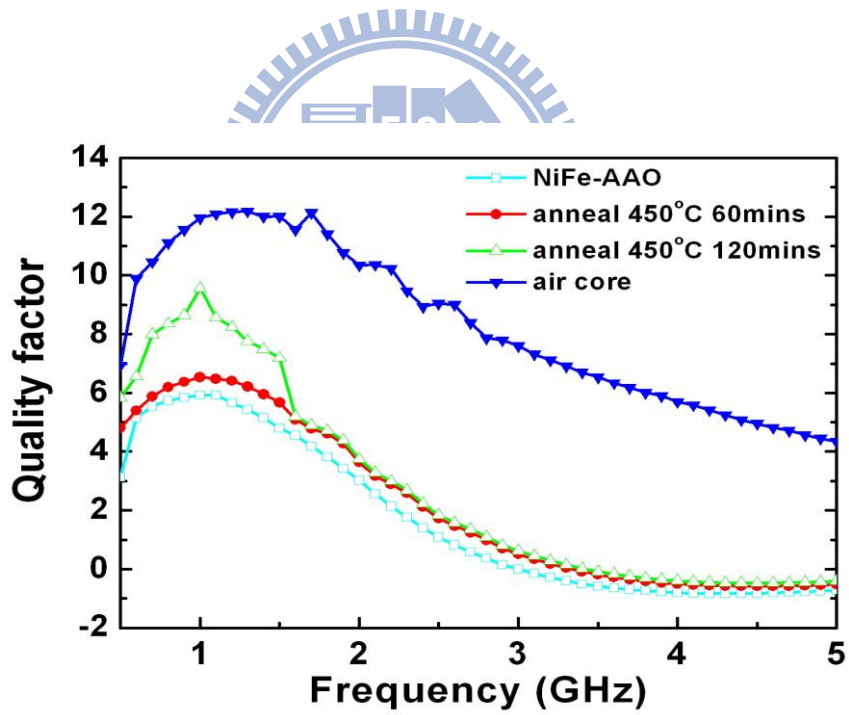
(b)

(c)

(d)

Fig.3-1. Measured high-frequency characteristics of spiral inductors with NiFe-AAO nanocomposite core. (a) Inductance of spiral inductor with N=3.5, d_{in}=100um. (b) Q-factor of spiral inductor with N=3.5, d_{in}=100um. (c) Inductance of spiral inductor with N=4.5, d_{in}=70um. (d) Q-factor of spiral inductor with N=4.5, d_{in}=70um.

Table 3-1
Inductance and Q-factor for different annealing time.

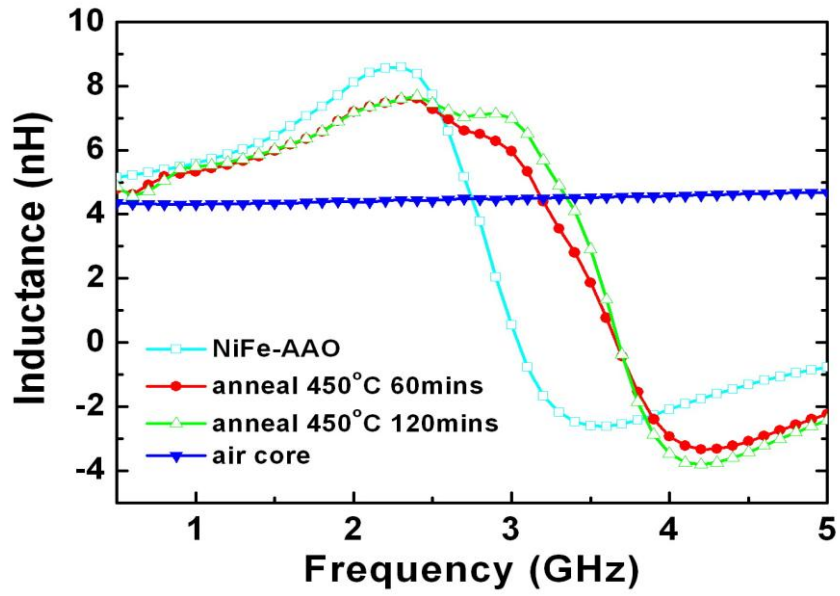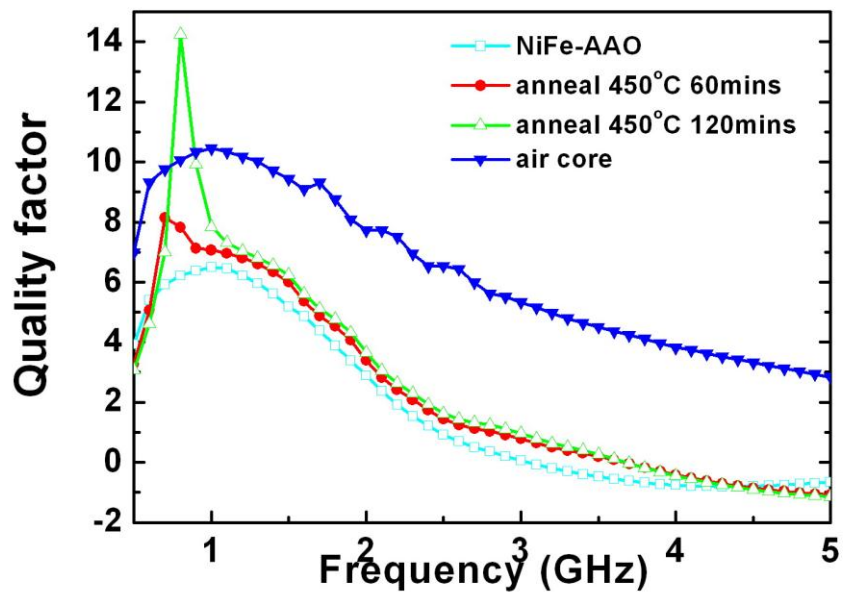| N	Types(inductor)	Inductance enhancement(up to 1 GHz)	f_{Qmax}(GHz)	Q_m
3.5	Air-core		1.3	12.1
	NiFe-AAO	25%	1	5.93
	anneal for 60 minutes	21.2%	1	6.53
	anneal for 120 minutes	21.5%	1.1	9.53
4.5	Air-core		1	10.4
	NiFe-AAO	23%	1	6.49
	anneal for 60 minutes	16.5%	0.7	8.14
	anneal for 120 minutes	16.6%	0.8	14.2

In order to verify the influence of thermal anneal on the inductor performance, the spiral inductors with NiFe-AAO nanocomposite magnetic core are annealed for two different time periods for 60 minutes and 120 minutes at 450 ℃, respectively. Fig. 8 shows the frequency dependence of the inductance and *Q*-factor of the fabricated inductors with NiFe-AAO nanocomposite magnetic core annealed for 60 minutes and 120 minutes, and the detailed parameter comparison between the inductor with and without thermal anneal samples as listed in Table 3-1. After annealing 60 minutes, the Q_m value of the spiral inductor of 3.5 turns with NiFe-AAO core has increased 10% (from 5.93 to 6.53), and after annealing 120 minutes, the Q_m value has increased 60% (from 5.93 to 9.53). Nevertheless, the inductance is accompanied with 4% decrease

(from 25% enhancement to 21% enhancement, up to 1 GHz). Similar Q enhancement and inductance degradation also occur in the case of the spiral inductor of 4.5 turns. After annealing 60 minutes, the Q_m value of the spiral inductor of 4.5 turns with NiFe-AAO core has increased 25% (from 6.49 to 8.14), and after annealing 120 minutes, the Q_m value has increased 118% (from 6.49 to 14.2). But, the inductance accompanies with 7% decrease (from 23% enhancement to 16% enhancement, up to 1 GHz), which the magnetic loss due to the higher coercive force (H_c) of the NiFe-AAO nanocomposite after annealing, as shown in Fig. 2-4.

As aforementioned, the Q degradation originated in the titanium which induced the effect of parasitic capacitance. By annealing to make a part of Ti (titanium) into TiO_x, however, Q-factor is a tradeoff of inductance decrease and magnetic loss. Although there is at least 23% inductance enhancement up 1 GHz in the work, the Q-factor can be further improved by thinning the layer of titanium and annealing enough time for more Ti into TiO_x, from a conducting layer to an insulation layer.Fig.3-3. and Fig.3-4. show the Smith chart of the inductor for S11.
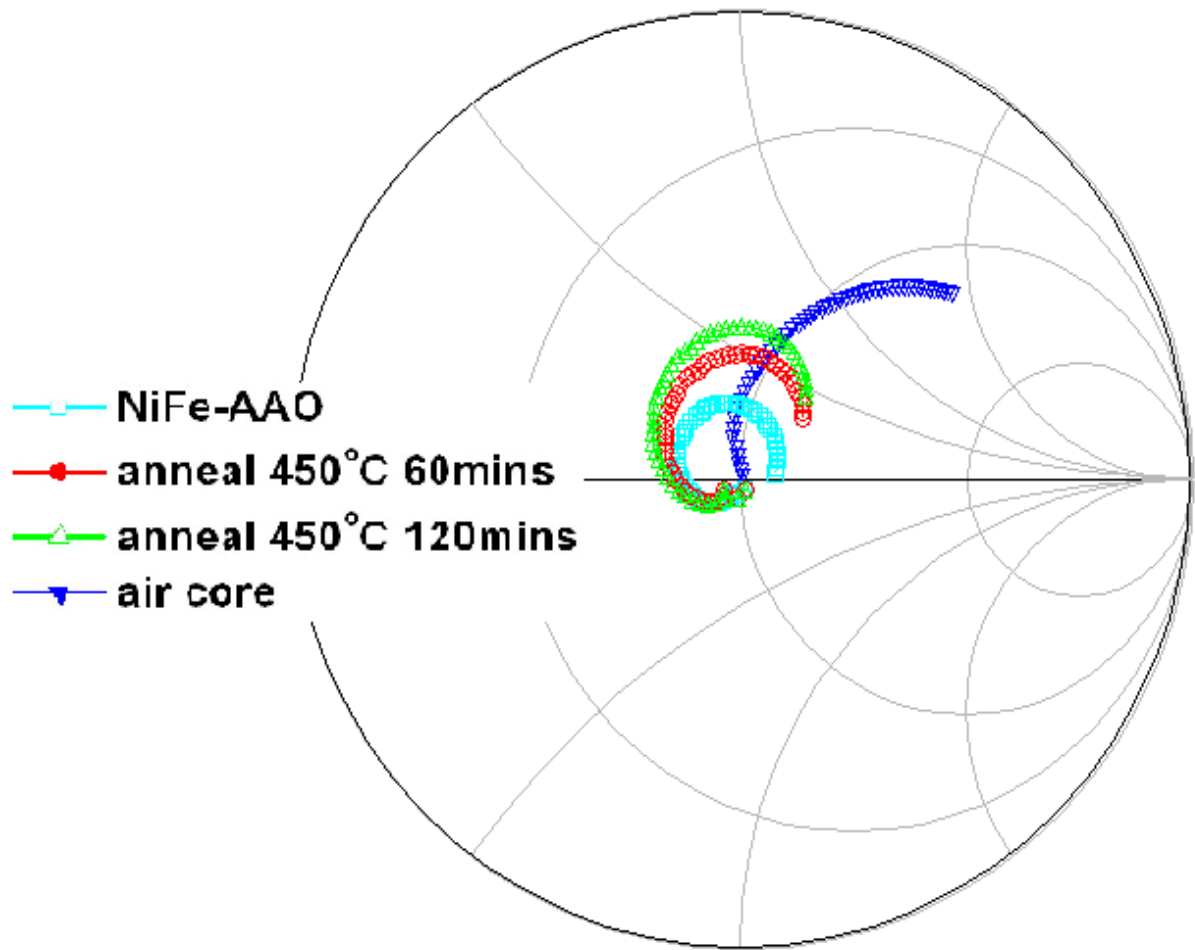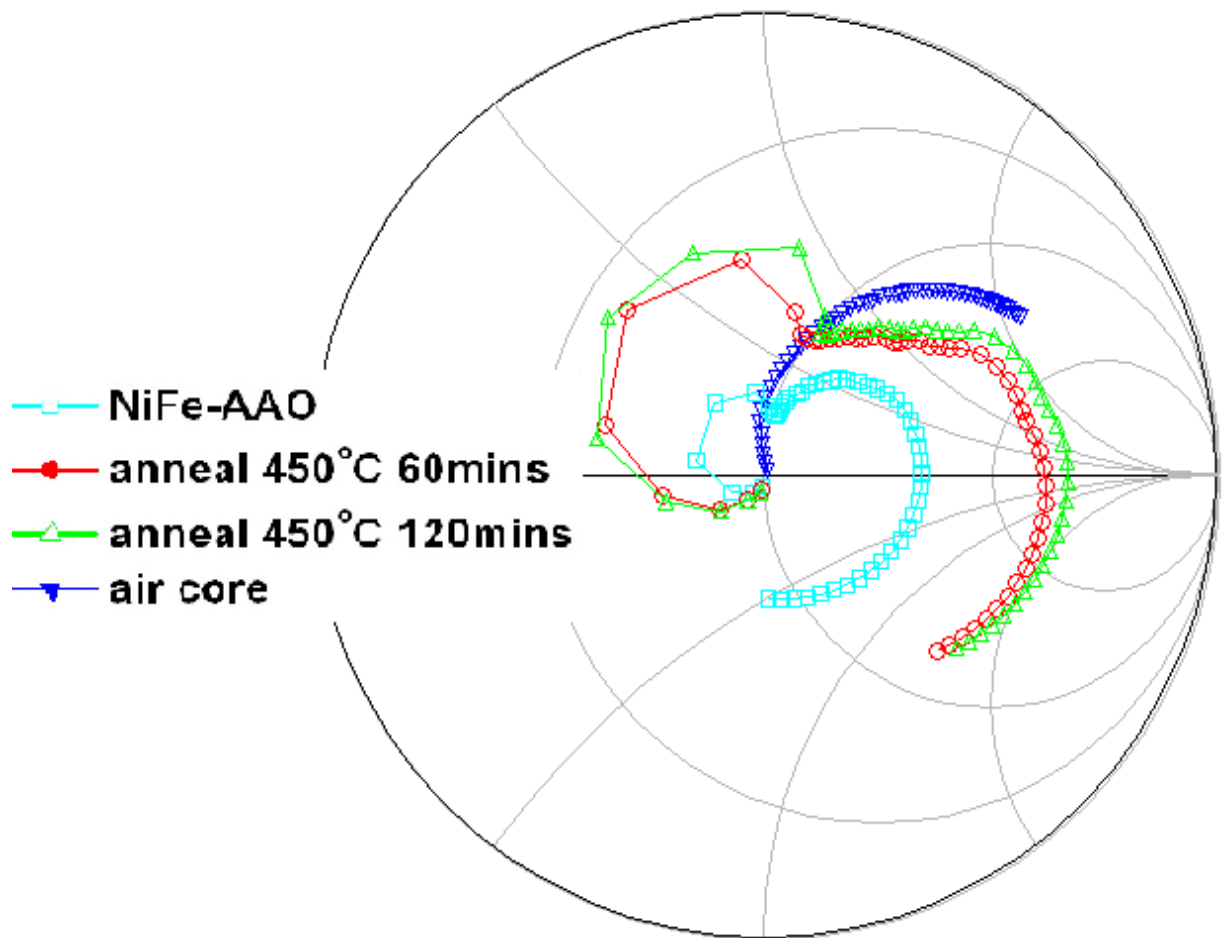
Fig.3-3. The S11 parameter of the 3.5 turns inductor.

Fig.3-4. The S11 parameter of the 4.5 turns inductor.

Chapter 4 Conclusion and Future Work

The ferromagnetic inductors using NiFe-AAO nanocomposite as magnetic core have fabricated. Incorporated with nanocomposite core, the 3.5 and 4.5-turn inductors can have improved inductance up 1 GHz and the nanocomposite (NiFe) has higher saturation magnetization and anisotropy magnetic field enabling a higher FMR frequency. Although the inductance has been effectively enhanced, the effect of capacitance resulted by titanium seed layer could cause the declination of Q that can be improved using thinner titanium or thermal anneal for the formation of titanium oxide for the effect resistance increase of the seed layer .

Reference

[1] I. J. Bahl, "High-performance inductors," *IEEE Trans. Microwave Theory Tech.*, Vol. 49, No. 4, pp. 654-664, Apr. 2001.

[2] S. Bantas and Y. Koutsoyannopoulos, "CMOS Active-LC Bandpass Filters With Coupled-Inductor Q-Enhancement and Center Frequency Tuning," *IEEE Trans. On circuits and systemss,* VOL. 51, NO. 2, Feb. 2004.

[3] B.Viala, A.S.Royet, R.Cuchet, M.Aid,P.Gaud, O.Valls, M.Ledieu, and O.Acher,"RF plane ferromagnetic inductors on silicon," *IEEE Trans.Magn.*, vol. 40, no. 4, pp. 1999–2001, July. 2004.

[4] J.Kim, W.Ni,C.Lee,Edwin C.Kan, Ian D.Hosein, Y.Song, and C.Liddell, "Magnetic property characterization of magnetite (Fe_3O_4) nanorod cores for integrated solenoid rf inductors," *J.Appl.Phys* 99. 08R903 (2006)

[5] R.F.Jiang,N.N.Shams,M.T.Rahman, and C. H. Lai, "Exchange-coupled IrMn/CoFe mulitlayers for RF-integrated inductors," *IEEE Trans.Magn.*, vol. 43, no. 10, pp. 3930–3932, Oct. 2007.

[6] M.C.Hsu, T.Y.Chao, Y.T.Cheng,C.M.Liu, and C.Chen, "The inductance enhancement study of spiral inductor using Ni-AAO nanocomposite core," *IEEE Trans.Nano.*, vol. 8. no.3, May 2009.

[7] C.C.Hu and A.Bai, "Influences of the phosphorus content on physicochemical properties of nickel–phosphorus deposits, " *Mater. Chem. Phys.* 77 (2002) 215–225.

[8] B.D. Cullity, Introduction to Magnetic Materials, Addison-Wesley, Reading, MA, 1972, pp. 31–136.

[9] N. Cordente, M. Respaud, F. Senocq, M. Casanove, C. Amiens, and B. Chaudret, "Synthesis and magnetic properties of nickel nanorods," *Nano Lett.*, vol. 1, pp. 565–568, 2001.

[10] S. Shingubara, "Fabrication of nanomaterials using porous alumina templates," *J. Nanopart. Res.*, vol. 5, pp. 17–30, 2003.

[11] M. M. Sinha and J. S. Kim, "Analysis of vibrational modes and phonon density of statesof aluminate spinels," *J. Korean Phys. Soc.*, vol. 43, no. 2, pp. 237–241, Aug. 2003.

[12] M.Tian, S.Xu, J.Wang, N.Kumar, E.Wertz, Q.Li, P.M.Campbell, M.H.W.Chan and T.E.Mallouk, " Penetrating the oxide barrier in situ and separating freestanding porous anodic alumina films in one step, " *Nano Letters*, 2005, Vol.5,No.4 697-703.

[13]   Rabin,O.;Herz,P.R.;Lin,Y.M.   ,Akinwande,A.I,Croniun,S.B.   and Dresselhaus,M.S. "Formation of thick porous anodic alumina films and nanowire   arrays   on   silicon   wafers   and glass , "*Adv.Funct.Mater*.2003,13,631.

[14] F.E Rasmussen, J.T Ravnkilde, P.T Tang, O.Hansen and S.Bouwstra, " Electroplating and characterization of cobalt-nickel-iron and nickel-iron for magnetic Microsystems applications, " *Sensors and Actuators A* 92 (2001) 242-248.

[15] H.Hamamura, H.Itoh, Y.Shimogaki, J.Aoyama, T.Yoshimi, J.Ueda and H.Komiyama, "Structure change of TiN/Ti/SiO$_2$ multilayers by N$_2$ annealing," *Thin Solid Film* 320 (1998) 31-34.

Vita

姓　　名：許欣富 (Hsin-Fu Hsu)

出生日期：中華民國七十三年二月十一日

出 生 地：新竹市

E - mail：marbury0320.ee96g@g2.nctu.edu.tw

學　　歷：

國立新竹高級中學　　　　　　　　　　　　(2000.9～2002.6)
(National HsinChu Senior High School)

國立中央大學大氣科學系　　　　　　　　　(2002.9～2007.6)
(Department of Physics, Nation Central University)

國立交通大學電子工程所碩士班　　　　　(2007.9～2009.9)
(Department of Electronics Engineering & Institute of Electronics,
 Nation Chiao Tung University)